JOURNAL OF SOLID STATE CHEMISTRY 98, 71–81 (1992)

Formation of Cu_3^{2+} Clusters: Structure, Bonding, and Topotactic Reactivity of Chalcogen Spinels $Cu_{1\pm y}Cr_2Se_3Br$

A. PAYER, M. SCHMALZ, W. PAULUS, AND R. SCHÖLLHORN*

Institut für Anorganische und Analytische Chemie, Technische Universität Berlin, D-1000 Berlin 12, Germany

R. SCHLÖGL

Institut für Anorganische Chemie, Universität Frankfurt, D-6000 Frankfurt/Main, Germany

AND C. RITTER

Institut Laue-Langevin, F-38042 Grenoble, France

Received July 25, 1991; in revised form October 25, 1991

The semiconducting chromium spinel $CuCr_2Se_3Br$ is shown to be accessible to reversible electrochemical and chemical reduction as well as to oxidation in Cu electrolytes by topotactic electron/ion transfer reactions leading to nonstoichiometric phases $Cu_{1+y}Cr_2Se_3Br$ ($0 \leq y \leq 0.50$) and $Cu_{1-y}CrSeBr$ ($0 \leq y \leq 0.23$). The oxidation proceeds under partial deintercalation of Cu and formation of valence band holes with a concurrent significant increase in the Curie temperatures T_c, which demonstrates the strong correlation between magnetic ordering and band hole concentration. The final product obtained by cathodic reduction is the new metastable spinel $Cu_{1.5}Cr_2Se_3Br$. Neutron diffraction and electron spectroscopy studies reveal that copper intercalation leads to the formation of Cu_3^{2+} clusters with electron defect bonding. Changes in the electronic structure upon reduction and oxidation processes are discussed on grounds of band structure schemes. © 1992 Academic Press, Inc.

Introduction

In our recent studies on the ferromagnetic metallic chalcogen spinels $CuCr_2X_4$ (X = S, Se, Te) we were able to show that the latter may undergo reversible topotactic redox reactions (*1–3*) of the type

$$CuCr_2X_4 + yCu^+ + ye^- \rightleftharpoons Cu_{1+y}Cr_2X_4 \quad (X = \text{S, Se, Te};\ 0 \leq y \leq 1). \quad (1)$$

This reaction proceeds via anion p band hole formation and annihilation, respectively. Partial isomorphous substitution of chalcogen anions by halide anions is known to result in spinels with the composition $CuCr_2X_3Y$ (X = chalcogen, Y = halogen) (*4*). Although the valence band is filled in these semiconducting compounds ($Cu^+(Cr^{3+})_2(X^{2-})_3Y^-$), we were able to demon-

---

* To whom correspondence should be addressed at Institut für Anorganische und Analytische Chemie, Technische Universität Berlin, Strasse des 17. Juni 135, D-1000 Berlin 12, Germany.

0022-4596/92 $5.00

strate by electrochemical and structural investigations of the selenium spinels $CuCr_2Se_3Br$ that this phase can be reduced, however, under uptake of Cu ions from aqueous or aprotic electrolytes to yield $Cu_{1.5}Cr_2Se_3Br$. Moreover, as opposed to the behavior of the parent phase $CuCr_2Se_4$, the halogen-substituted phase can also be oxidized partially to $Cu_{0.77}Cr_2Se_3Br$ with a simultaneous significant increase in the Curie temperature. We report here on the formation and characterisation of these compounds and their interesting features concerning structure, electronic properties, and chemical bonding.

Experimental

The preparation of $CuCr_2Se_3Br$ was carried out by heating Cr, Se, and CuBr with appropriate stoichiometry in an evacuated silica ampoule for 10–14 days at 1000 K with subsequent slow cooling. The products of the thermal and the electrochemical reactions were structurally characterized by X-ray powder diffraction and analyzed chemically by atomic absorption spectroscopy (AAS).

The potential/charge transfer diagrams of the electrochemical reactions were obtained under dynamic (galvanostatic) and equilibrium (potentiostatic) conditions using aqueous $CuSO_4$ or aprotic $CuCl/CH_3CN$ solutions as electrolytes. In order to determine the Curie temperatures (T_c) the temperature dependence of the magnetic susceptibility (Curie–Weiss law) was measured with a Faraday balance.

The structure of $Cu_{1.5}Cr_2Se_3Br$ was obtained from neutron powder data using Rietveld refinement methods (D2B, Institute Laue-Langevin (ILL) in Grenoble, France; $\lambda = 1.59$ Å, $\sin \Theta/\lambda \leq 0.6$). Photoelectron spectra of the intercalation compound $Cu_{1.5}Cr_2Se_3Br$ and the reference materials $CuCr_2Se_3Br$ and elemental copper were obtained by exciting the core levels (XPS) with Mg*Kα* radiation (1254 eV) and the valence energy bands (UPS) with ultraviolet light (He(I): 21.4 eV; He(II): 40.8 eV) (*2*). In order to protect the samples from surface oxidation, materials were kept under inert gas atmosphere and the reaction ampoules were opened immediately before introducing the sample into the spectrometer. A mechanical device was used to scrape the crystallite surface *in situ* until no oxygen surface contamination was detectable in survey spectra. The applied cleaning technique of sputtering usually leads to rapid disintegration of the compounds under investigation.

Results and Discussion

The *oxidation* of samples of $CuCr_2Se_3Br$ was performed by electrochemical as well as by chemical means. The anodic oxidation of pressed polycrystalline working electrodes at 300 K in acid electrolytes (0.1 N H_2SO_4) was performed under galvanostatic conditions until the potential of oxygen formation was reached. The presence of small amounts of elemental Se in the reaction product indicates that the deintercalation of copper ions from the solid competes with a slow oxidative decomposition of the host lattice at higher oxidation potentials. From the Cu/Cr ratio the lower phase limit of $Cu_{1-y}C_2Se_3Br$ was determined as $y = 0.23$, which is well in agreement with literature data for the corresponding thermal phases ($y = 0.22$) (*5*). The chemical oxidation with I_2 in acetonitrile at 300 K yielded identical products: $Cu_{0.77}Cr_2Se_3Br$ is cubic with $a_0 = 1037.4$ pm. The oxidation process at $0 \leq y \leq 0.23$ corresponds to a one-phase region with a continuous change in the lattice parameter a_0 (Fig. 1).

As discussed above the *reduction* of $CuCr_2Se_3Br$ under uptake of copper ions should not be expected since $[Cr_2Se_4]^{2-}$ and $[Cr_2Se_3Br]^-$ are isoelectronic and do not have p band holes. The potential/charge transfer diagram for the galvanostatic ca-

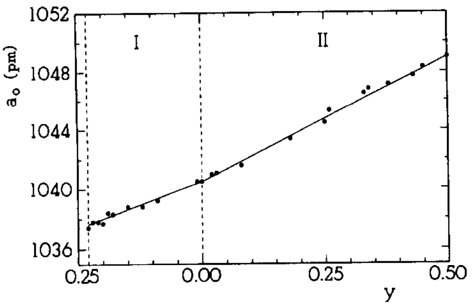

FIG. 1. Cubic lattice parameter a_0 in dependence on the stoichiometric index y. (I) $Cu_{1-y}Cr_2Se_3Br$ (oxidation of $CuCr_2Se_3Br$); (II) $Cu_{1+y}Cr_2Se_3Br$ (reduction of $CuCr_2Se_3Br$).

thodic reduction of $CuCr_2Se_3Br$ electrodes in 0.25 M $CuCl/CH_3CN$, which is shown in Fig. 2, clearly demonstrates, however, a continuous decrease in potential with increasing charge transfer. The endpoint of the reaction is reached with the potential of copper metal deposition after a charge transfer of 0.5 $e^-/CuCr_2Se_3Br$. The electrochemical reduction can similarly be performed in aqueous electrolyte (0.5 M $CuSO_4/H_2SO_4$) which requires a charge transfer of 1.0 $e^-/CuCr_2Se_3Br$ due to the presence of bivalent copper ions in the electrolyte. The composition of the end product as calculated from the electrochemical data is thus $Cu_{1.5}Cr_2Se_3Br$; this value was confirmed by elemental analysis. Electrochemical reduction with different current densities as well as reduction in short circuit cells yielded cubic end products with identical stoichiometry and lattice parameters a_0 = 1049.0 pm. The reduction process is again corresponding to a one-phase region at $0 \leq y \leq 0.5$ which is demonstrated by the continuous change in lattice parameter a_0 as a function of y (Fig. 1). The lattice parameter changes with the stoichiometry are almost linear for the reduction as well as for the oxidation process; the slope of the two curve sections are slightly different.

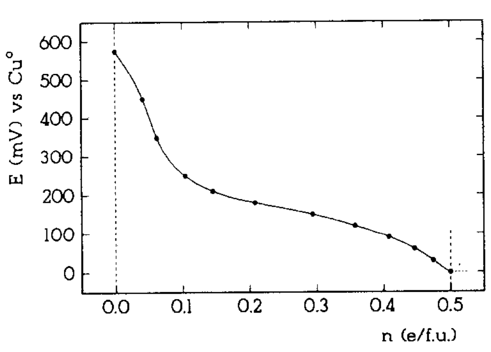

FIG. 2. Potential (E)/charge transfer (n) diagram for the potentiostatic reduction of $CuCr_2Se_3Br$ (polycrystalline sample pressed into a platinum net) in 0.25 M $CuCl/CH_3CN$ electrolyte. Values indicated by closed circles (●) have been obtained independently by the potentiostatic reaction mode.

Oxidation and reduction of $CuCr_2Se_3Br$ both are reversible topotactic electron/ion transfer processes and can be described by the following equations:

Reduction

$$CuCr_2Se_3Br + y \cdot Cu^+ + y \cdot e^- \rightleftharpoons Cu_{1+y}Cr_2Se_3Br \quad (0 \leq y \leq 0.50) \quad (2a)$$

Oxidation

$$CuCr_2Se_3Br \rightleftharpoons Cu_{1-y}Cr_2Se_3Br + y \cdot Cu^+ + y \cdot e^- \quad (0 \leq y \leq 0.23). \quad (2b)$$

Attempts to prepare $Cu_{1.5}Cr_2Se_3Br$ by thermal reaction from the elements, from $CuCr_2Se_3Br$ and copper metal or from mixtures of Cu, CuBr, Cr, and Se in appropriate ratios at 900–1100 K failed. The reaction products identified in the latter case were hexagonal $CuCrSe_2$ and $CrBr_2$:

$$Cu + 2CuBr + 4Cr + 6Se \rightarrow 3CuCrSe_2 + CrBr_2. \quad (3)$$

It is to be concluded therefore that $Cu_{1.5}Cr_2Se_3Br$ prepared at low temperature is a metastable phase that cannot be obtained by thermal reaction.

In order to determine the structure of the new phase $Cu_{1.5}Cr_2Se_3Br$, particularly with respect to the location of the excess copper ions, we decided to perform a powder neutron diffraction study. The structure of the parent lattice $CuCr_2Se_3Br$ can be described as a spinel base compound (space group $Fd\bar{3}m$) with cubic anion packing (Se and Br statistically on 32*e*), chromium on octahedral sites (16*d*), and copper on tetrahedral sites (8*a*). Unoccupied tetrahedral (48*f*, 8*b*) and octahedral (16*c*) sites are basically available for the location of excess copper ions.

The sample used for neutron diffraction consisted of a series of smaller batches prepared electrochemically. Each batch was checked separately for stoichiometry and lattice parameters (X-ray Guinier technique). A few low intensity additional lines were observed, which could be indexed on the base of a hexagonal lattice; they were identified as belonging to the hexagonal modification of $CuCrSe_2$. The wavelength used was 1.59 Å with a scattering angle between 10° and 150° (2Θ). Neutron scattering factors were taken from (*6*); the angular dependent magnetic scattering amplitude for the Cr^{3+} ions is reported in (*7*).

For the excess copper ions intercalated into the parent phase $CuCr_2Se_3Br$ copper tetrahedral sites (48*f*, 8*b*) as well as octahedral sites (16*c*) are available. The refinement of the nonmagnetic 300K basic structure of $Cu_{1.5}Cr_2Se_2Br$ shows that no additional copper is intercalated on the tetrahedral 8*b* and 48*f* sites, whereas a partial occupation of about 0.15 per formula unit can be located on the 16*c* octahedral sites. The occupation of this position seems to be rather unlikely, since it implies a next copper–copper distance of 227 pm, which is rather short as compared to copper metal, where 255 pm is found for the next nearest neighbor distance. As a consequence a repulsion within this linear Cu_3 arrangement should occur, giving rise to shift displacements of the intercalated copper atoms away from the ideal octahedral positions.

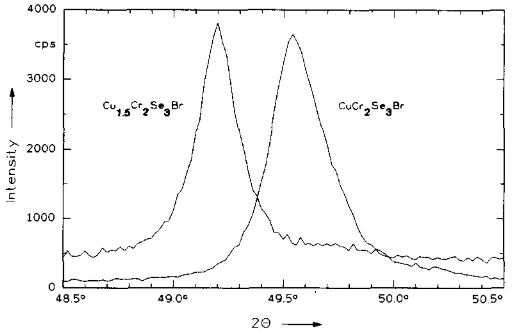

FIG. 3. Comparison of the XRD peak profile of the [400] reflection of the host lattice $CuCr_2Se_3Br$ and the intercalation compound $Cu_{1.5}Cr_2Se_3Br$.

From the low occupation density of only 0.15 Cu/f.u. together with an unusual high temperature factor, displacements of the copper atoms from the center of the octahedral hole have to be assumed which, however, occur somewhat statistically. As no additional lines or line broadening can be derived from neutron or X-ray powder diffraction, a lowering of the symmetry was first assumed to be improbable. For comparison the (4 0 0) reflection of $CuCr_2Se_3Br$ and of $Cu_{1.5}Cr_2Se_3Br$ are shown in Fig. 3, where no significant increase of the FWHM is evident.

A new model for the distribution of the intercalated copper was assumed therefore within the spinel group $Fd\bar{3}m$, which allows the displacements of the intercalated copper perpendicular to the connection line between two neighboring Cu atoms with tetrahedral coordination (8*a*). As a consequence of the cubic symmetry the ideal center of the octahedral position between the two tetrahedra then splits into six equivalent positions forming on the 96 *h* sites a planar hexagon which is statistically occupied (Fig. 4). The displacements were refined to be exactly 100 pm from the center of symmetry. This was made under the assumption of 0.5 Cu/f.u., which is the total amount of the intercalated copper being located on that site. Obviously, there is a strong correlation between the temperature factor and the oc-

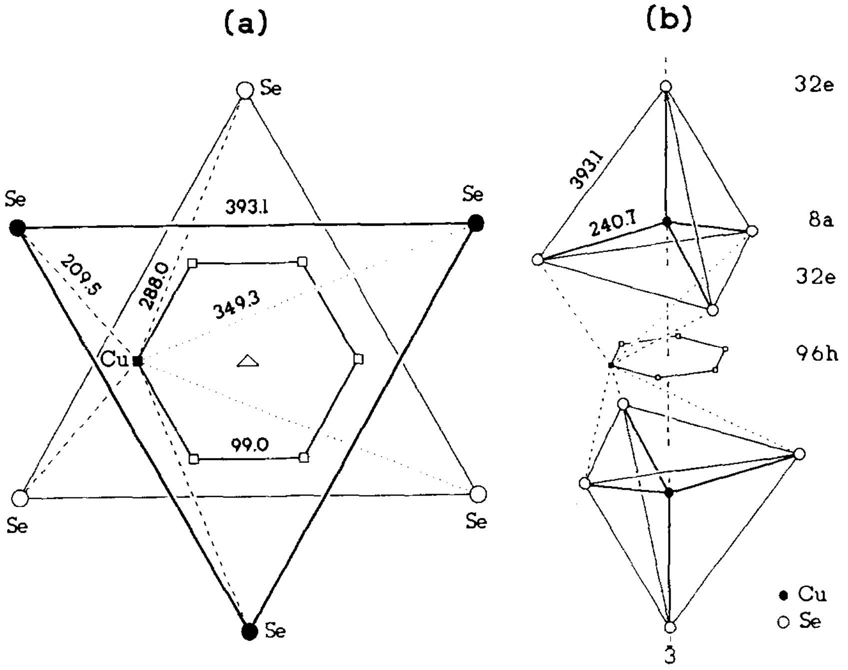

FIG. 4. Position of the (96h) hexagon inside the Se_6 octahedron (atomic distances are given in pm). (a) View along the threefold axis Δ: Cu (8*a*) atoms on the threefold axis above and beneath Δ. (b) View perpendicular to the threefold axis.

cupation density in the case of the 96 *h* position, still resulting in a high but not unreasonable route mean square amplitude of the copper motion. The use of anisotropic temperature factors did result neither in better profile refinements nor in a better understanding of the copper disorder. As can be seen from the structure data in Table I the temperature amplitude of the tetrahedrally coordinated copper is also about four times higher compared to that of the chromium ions, which in addition to the copper ordering discussed above gives rise to local disorder. This can be regarded as a consequence of the short Cu–Cu distances in the Cu_3 unit. In Fig. 5 the plot of the Rietveld refinement is presented.

TABLE I

STRUCTURAL PARAMETERS OF $Cu_{1.5}Cr_2Se_3Br$ AT 295 K

Atom		*x*	*y*	*z*	*B*	*N*
Se	32*e*	0.2575(3)	0.2575(3)	0.2575(3)	1.07(3)	3.00
Br	32*e*	0.2575(3)	0.2575(3)	0.2575(3)	1.07(3)	1.00
Cr	16*d*	$\frac{1}{2}$	$\frac{1}{2}$	$\frac{1}{2}$	1.14(3)	2.00
Cu(1)	8*a*	$\frac{1}{8}$	$\frac{1}{8}$	$\frac{1}{8}$	3.92(6)	1.00
Cu(2)	96*h*	0	0.067(1)	−0.067(1)	10(1)	0.50

Note. a = 1049.02(2) pm; R_F = 5.49%; N, occupation factor [atoms/f.u.]; B, isotropic temperature factor.

Cooling $Cu_{1.5}Cr_2Se_3Br$ down to low temperatures causes a ferromagnetic ordering at a T_c of 170 K. The structure determination at 1.5 K is still a problem as a consequence of copper disorder, although the copper motion should have ceased. The temperature factors for the additional copper ions are still too high, combined with an inaccuracy in the refinement of the y-parameter for the 96*h* copper position, varying between 0 and 0.055. Although the structure data of the

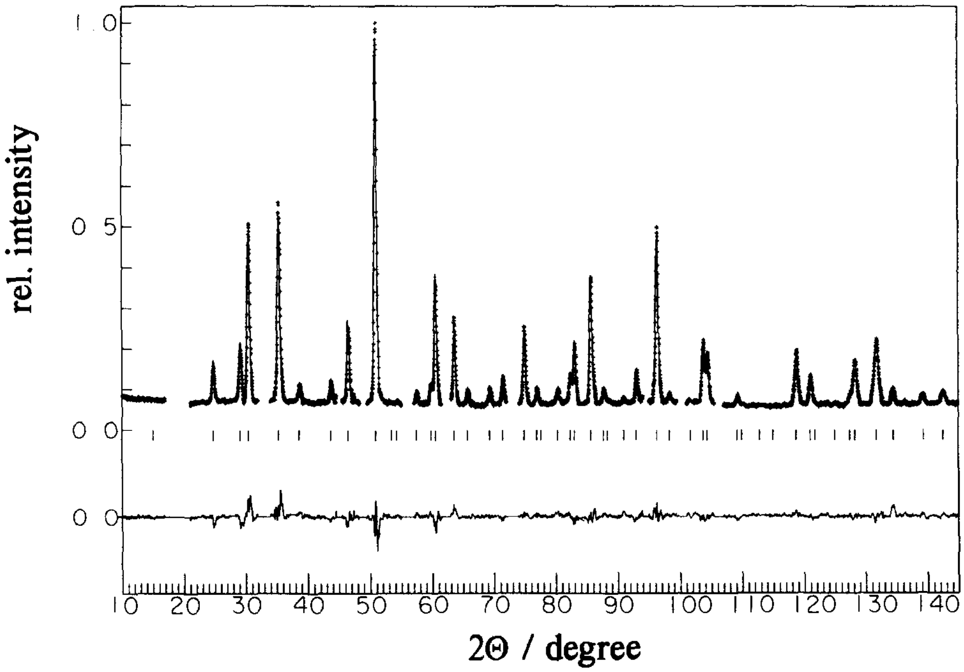

FIG. 5. Rietveld profile refinement for the neutron diffractogram of $Cu_{1.5}Cr_2Se_3Br$ at 295 K. The calculated curve is presented by a solid line; the data points are shown as crosses. At the bottom the peak positions and the difference plot are indicated.

other atoms do not vary upon cooling—except that the temperature amplitude of all basic atoms is only half the value of the 300 K structure—we were not able to determine the exact copper positions. At higher temperatures the copper disorder can be compensated by the thermal motion, while the copper positions can be localized. For the refinement at 1.5 K we assume thus the displacement of the intercalated copper atom to be basically the same as that for the room temperature refined structure. As a consequence of the ferromagnetic ordering at lower temperatures (T_c = 170 K) we obtained a magnetic moment of 2.97 ± 0.06 μ_B on the chromium positions corresponding to the spin-only value of Cr^{3+} ($3d^3$).

TABLE II

INTERATOMIC DISTANCES IN $CuCr_2Se_3Br$ AND $Cu_{1.5}Cr_2Se_3Br$ IN [pm]

	$CuCr_2Se_3Br^a$	$Cu_{1.5}Cr_2Se_3Br$
Cu(1)-Cu(1)	450.6	454.2
Cu(1)-Cu(2)		247.9(9)
[16c]-Cu(2)		99(1)
Cu(1)-Se	250.5	240.7(3)
Cu(2)-Se		2× 209.5(9)
		2× 288.0(5)
		2× 349.3(9)
Cr-Se	246.4	254.6(3)
Se-Se	409.1	393.1(4)

[a] a_0 = 1040.5 pm; x (32e) = 0.264, Ref. (*10*).

With respect to the anion coordination of the excess copper on each of the hexagon positions the cations are located inside a distorted CuX_4 tetrahedron (2 × 2 Cu–X distances; cf. Table II) given by the four nearest anions (two other anions are too far away). This environment is caused by the strongly chalcophilic character of the copper ions and covalent Cu–X bonding resulting in a tendency to reach shorter Cu–X distances and a preference for tetrahedral

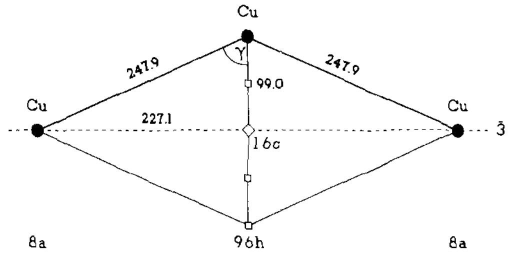

FIG. 6. Positions of the copper atoms in the Cu_3 cluster in $Cu_{1.5}Cr_2Se_3Br$; view perpendicular to the threefold axis and the hexagon plane (atomic distances in pm; $\gamma = 67.5°$).

coordination. The unusual short Cu–Cu distances force the excess copper ions to leave the center of the CuX_6 octahedron (16*c*) and lead to a split position on a plane hexagon perpendicular to the threefold axis corresponding to the connection line of the two neighboring Cu (8*a*) atoms, as can be seen in Fig. 6.

From the electronic point of view this structure model is similarly plausible. The occupation of the tetrahedral sites (48*f*, 8*b*) by copper would imply an uptake of electrons by the chromium anion band and the reduction of Cr^{3+} to Cr^{2+}, which is most unlikely because of the low redox potential. The formation of Cu–Cu bonds would be a possible alternative. The localization of copper on the 96*h* positions with Cu–Cu distances of 248 pm (255 pm in copper metal) meets the structural requirements for the model (local ionic picture) of an angular Cu_3^{2+} cluster unit (Fig. 6) with three center electron defect metal/metal bonding. In order to verify this assumption photoelectron spectroscopy (XPS) was used to determine the binding energies of Cu 2*p*, Cr 2*p*, and Se 3*d* in $Cu_{1.5}Cr_2Se_3Br$ in comparison with those of the host lattice $CuCr_2Se_3Br$ and elemental Cu^0.

The determination of the composition of $Cu_{1.5}Cr_2Se_3Br$ at the surface indicated an excess of copper. A negative gradient of the Cu concentration from the surface into the bulk of the material may be the consequence of the electrochemical synthesis method (gradients in a very thin surface layer). The incorporation process of Cu into a dense structure will be strongly diffusion controlled, leading within the limited time of the electrochemical experiment to a pseudo-equilibrium. All bulk analytical methods will thus determine an average Cu value which may be different from that of the surface region.

In Fig. 7 we can recognize that the Cu 2*p* peaks exhibit a chemical shift and a line broadening for $Cu_{1.5}Cr_2Se_3Br$ relative to Cu metal and to the host compound. The Madelung shift contribution to the binding energy (b.e.) is assumed to be small because of the identical anion lattices in both spinel compounds. Excluding segregated copper metal and Cu^{2+} impurities because of the observed shift and the missing shake-up satellites, we can conclude the presence of a new copper species. UPS measurements (Fig. 8)

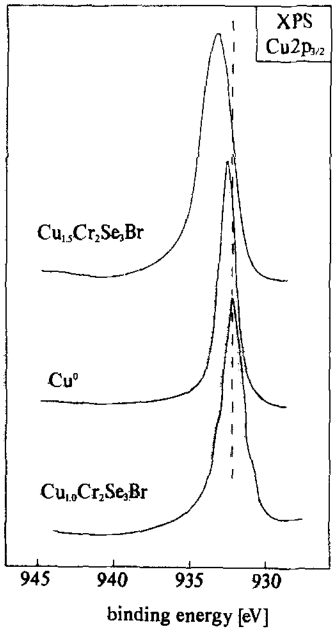

FIG. 7. XPS Cu $2p_{3/2}$ spectra of $Cu_{1.5}Cr_2Se_3Br$, Cu^0, and $CuCr_2Se_3Br$.

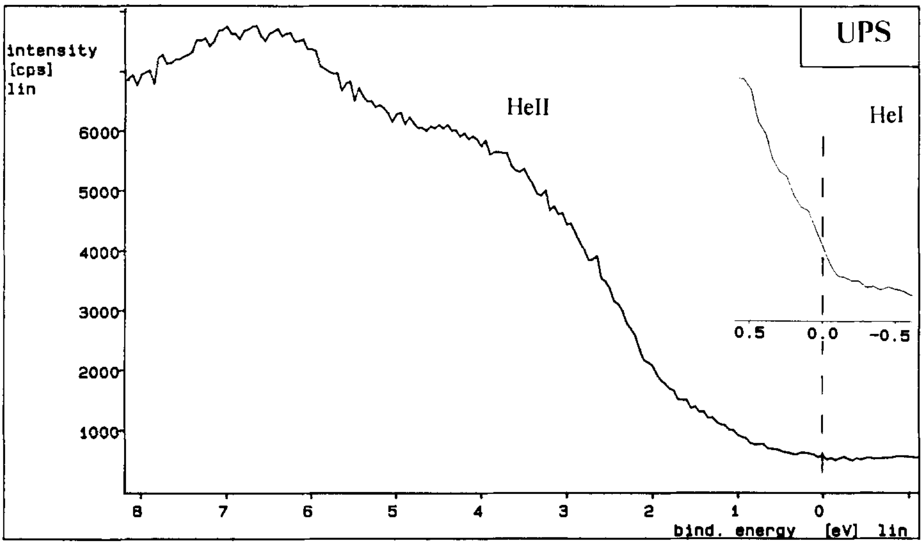

FIG. 8. He(I) and He(II) UPS spectra of $Cu_{1.5}Cr_2Se_3Br$.

showed a low electron density at the Fermi level and a small Fermi edge feature. $Cu_{1.5}Cr_2Se_3Br$ can thus be considered a metal and we can exclude electrostatic charging of the sample. The higher binding energy for the $Cu_{1.5}$ phase can be explained by the formation of a new valence band at the Fermi level. From the magnetic data, which show no significant change of the Curie temperature T_c (see below), we conclude that the chromium-anion band remains unchanged, excluding an electron exchange between the parent valence band and the new band. As demonstrated in Fig. 9, we further assume that the new band is probably formed by the Cu 3*d*/4*s* orbitals arising from the copper–copper interactions in the $Cu_{1.5}Cr_2Se_2Br$ compound. Although it can be derived from Fig. 8 (expansion of the He(I) plot) that only a low electron density at the Fermi level exists, the effect of the new band on the binding energies of all the core levels is significant (see Table III). This effect, called "Fermi level pinning" also provides for a shift of the core levels of the other atomic species, whereby the difference in position for Cr, Se, and Br remains constant. This is a reflection of the intercalation process, because the combination of atomic orbitals in a metallic compound leads to band structures which belong to all atoms in the solid crystal structure.

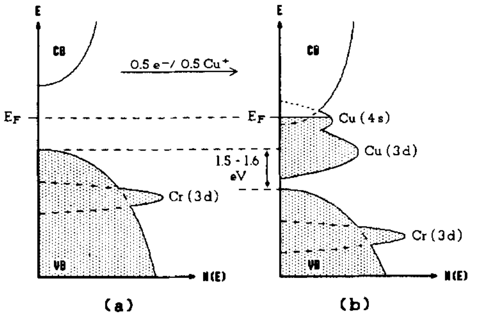

FIG. 9. Band schemes of $CuCr_2Se_3Br$ (a) and $Cu_{1.5}Cr_2Se_2Br$ (b), demonstrating the "Fermi level pinning" and the formation of the new copper band in $Cu_{1.5}Cr_2Se_3Br$ after reduction of $CuCr_2Se_3Br$ in the Cu^+ electrolyte. (*E*, energy; *N*(*E*), density of states; VB, valence band; CB, conduction band; E_F, Fermi energy; occupied states are stippled).

The Fermi level pinning is a spectroscopic artifact. The position of the core levels is relative to the Fermi edge; the latter itself is assumed to remain fixed relative to the

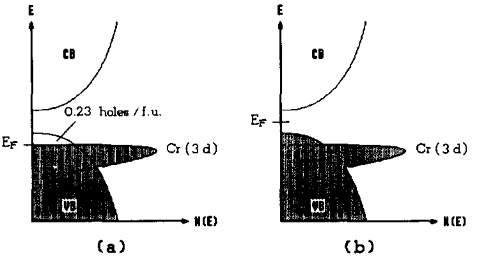

FIG. 10. Band schemes of $Cu_{0.77}Cr_2Se_3Br$ (a) and $CuCr_2Se_3Br$ (b).

vacuum level. Similar effects were detected in UPS He(I) spectra of graphite intercalation compounds (GIC) by Schlögl (*8*), where the valence band spectra of pristine graphite and a typical donor GIC (C_8Rb) were compared. The GIC shows a new peak at the Fermi edge, which closely resembles the conduction band feature of pure alkali metals. This peak accounts for a shift of all other characteristic peak structures for the value of the width of the new band of about 1.0–1.5 eV, when the Fermi level is pinned.

In agreement with the UPS results a band structure for $Cu_{1.5}Cr_2Se_3Br$ is suggested leading to metallic behavior, whereas that for the host $CuCr_2Se_3Br$ must correspond to semiconducting behavior. The binding energies of the core levels of the different atoms are given in Table III. In contrast to the other species the difference in the b.e. of Cu $2p$ between $CuCr_2Se_3Br$ and $Cu_{1.5}Cr_2Se_3Br$ is smaller (1.1 eV instead of 1.5–1.6 eV). The observed small negative shift is ascribed to the changeover from a semiconducting to a metallic matrix caused by a copper–copper interaction.

The line shape of the Cu $2p$ peaks in $Cu_{1.5}Cr_2Se_3Br$ is slightly asymmetric and broadened. The Cu $2p_{3/2}$ peak was fitted to two components. The main species at 933.4 eV was attributed to the new copper species, whereas the peak at 936.5 eV was attributed to a small satellite of the main signal. A change of the linewidth was also observed at the Se $3d$ spectrum of the intercalated compound which is again attributed to the semiconductor–metal transition.

The change of electronic properties was simultaneously investigated by magnetic measurements. The Curie temperature of $Cu_{1.5}Cr_2Se_3Br$ (T_c = 170 K) is nearly the same as in $CuCr_2Se_3Br$ (190 K, cf. Table IV). The ferromagnetism of the chromium chalcogen spinels results from the ferromagnetic coupling between the chromium cations and the anions (90° CrXCr superexchange), whereby the strength of these interactions is dependent on the hole concentration in the v.b. responsible for the electronic conductivity.

Metallic conducting $CuCr_2X_4$ (X = S, Se, Te) phases exhibit 1 hole/f.u. (*2*) in the valence band combined with high Curie temperatures. The reduction of the valence band holes by intercalation of Cu^+/e^-, partial substitution of Cu^+ by A^{2+} cations (Cd, Hg, Zn) or of selenium by bromine, respectively, leads finally to semiconducting spinel

TABLE III

BINDING ENERGIES [eV] OF CORE ELECTRONS

	Cu $2p_{3/2}$	Cr $2p_{3/2}$	Br $3p_{3/2}$	Se $3d_{3/2}$
Cu^0	932.6			
$Cu_{1.0}Cr_2Se_3Br$	932.3	574.6	181.6	53.2
$Cu_{1.5}Cr_2Se_3Br$	933.4	576.1	183.2	54.7
Difference	+1.1	+1.5	+1.6	+1.5

TABLE IV

CURIE TEMPERATURES (T_c) FOR $Cu_{1+y}Cr_2Se_3Br$ PHASES

$1 + y$	T_c (K)
0.8	320 ± 10
1.0	190[a]
1.5	170 ± 10

[a] Ref. (*11*).

compounds with low Curie temperatures ($T_c < 200$ K) where the valence band is filled.

The uptake of electrons by intercalating copper into $CuCr_2Se_3Br$ has no influence on the electronic configuration of the Cr–X sublattice, but the electrons are delocalized in interacting Cu_3^{2+} clusters forming the new band above the valence band. In the case in which this new band would overlap with the valence band or even, according to Folmer and Jellinek (*12*), would lie far below the top of the valence band creating holes, these holes should enhance the ferromagnetic coupling. Since T_c does not change significantly, we conclude that a band gap exists between the valence band and the copper band. The slight decrease of T_c is attributed to the expansion of the spinel lattice, since increasing Cr–Se distances will cause a weakening of the ferromagnetic coupling.

On the other hand, the oxidation of $CuCr_2Se_3Br$ increases the Curie temperatures significantly as a result of the removal of electrons from the valence band leading to v.b. holes. As opposed to $Cu_{1+y}Cr_2X_4$ (X = S, Se, Te; $0 \leq y \leq 1$) (*1*) the lower phase limit is reached for $Cu_{1-y}Cr_2Se_3Br$ at $y = 0.23$. From the structural point of view it should be possible to deintercalate the copper completely analogous to the oxidation of the spinel $CuTi_2S_4$ which yields cubic TiS_2 (*9*) so that there must be electronic reasons for the observed behavior. One possible explanation is a modified band structure of $CuCr_2X_4$, which changes by partial substitution of selenium by bromine (Figs. 10a and 10b). While in $CuCr_2X_4$ the Fermi level is of the same energy as the top of the Cr 3*d* band only when reaching the concentration of 1 v.b. hole/f.u., this is already the case for the bromine spinel at the stoichiometry $Cu_{0.77}Cr_2Se_2Br$ ($\triangleq$ 0.23 holes/f.u.). Obviously, a rather high redox potential exists for further oxidation corresponding to the removal of electrons from the Cr 3*d* band with the formal oxidation of Cr^{3+} to Cr^{4+}. Since the redox potential of Se^{2-}/Se^0 is much lower, decomposition of the spinel lattice and segregation of elemental selenium take place.

Conclusions

The reversible reactions performed in the oxidation range $0 \leq y \leq 0.23$ for $Cu_{1-y}Cr_2Se_3Br$ correspond to band hole generation and annihilation by chemical reactions at ambient temperatures and demonstrate that this concept (*1–3*) is a useful base for the control of the electronic properties of solids. In particular it shows again that there is a strong correlation between the ground state hole concentration and the temperature dependence of the magnetic ordering states, i.e., the strength of spin coupling.

In the metastable new phase $Cu_{1.5}Cr_2Se_3Br$ the electron/ion transfer reaction is unique, since the electron is not transferred to the host lattice but remains bound in Cu/Cu interaction states. A related situation with a three-center electron defect bonding has been reported by us earlier for the Chevrel phase $Li_3Mo_6S_8$, where partial charge transfer to the host lattice with the appearance of Li_3^{2+} clusters has been observed, although the valence band is not filled in the latter case (*13*). Since the electron in $Cu_{1.5}Cr_2Se_3Br$ is not transferred to the host lattice, there is no effect on the chromium/anion band and thus no effect on the strength of the ferromagnetic coupling.

Acknowledgments

Support of this work by the Deutsche Forschungsgemeinschaft, the Bundesministerium für Forschung und Technologie, and the Fritz-Haber-Institut der Max-Planck-Gesellschaft is gratefully acknowledged.

References

1. R. SCHÖLLHORN AND A. PAYER, *Angew. Chem.* **98,** 895 (1986); *Angew. Chem. Int. Ed. Engl.* **25,** 905 (1986).

2. A. PAYER, M. SCHMALZ, R. SCHÖLLHORN, R. SCHLÖGL, AND C. RITTER, *Mater. Res. Bull.* **25,** 515 (1990).

3. R. SCHÖLLHORN, *Solid State Ionics* **32/33,** 23 (1989).

4. R. P. VAN STAPELE, *in* "Ferromagnetic Materials" (E. P. Wohlfarth, Ed.), Vol. 3, 603, North Holland, Amsterdam (1982).

5. H. PINK, W. K. UNGER, H. SCHAEFER, AND H. GOEBEL, *Appl. Phys.* **4,** 147 (1974).

6. H. M. RIETVELD, *Acta Cryst.* **22,** 151 (1967); *J. Appl. Crystallogr.* **2,** 65 (1969).

7. R. E. WATSON AND A. J. FREEMAN, *Acta Crystallogr.* **14,** 27 (1961).

8. R. SCHLÖGL, "Experimental Electronic Structure of GIC," Springer-Verlag, Berlin (in print).

9. R. SCHÖLLHORN AND A. PAYER, *Angew. Chem.* **97,** 57 (1985); *Angew. Chem. Int. Ed. Engl.* **24,** 67 (1985).

10. J. G. WHITE AND M. ROBBINS, *J. Appl. Phys.* **39,** 664 (1968).

11. K. MIYATANI, K. MINEMATSU, Y. WADA, F. OKAMOTO, K. KATO, AND P. K. BALTZER, *J. Phys. Chem. Solids* **32,** 1429 (1971).

12. J. C. W. FOLMER AND F. JELLINEK, *J. Less-Common Met.* **76,** 153 (1980).

13. E. GOCKE, R. SCHÖLLHORN, G. ASELMANN AND W. MÜLLER-WARMUTH, *Inorg. Chem* **26,** 1805 (1987).